Bull Volcanol (2007) 70:105–113
DOI 10.1007/s00445-007-0123-8

SHORT SCIENTIFIC COMMUNICATION

Eruptive styles and inferences about plumbing systems at Hidden Cone and Little Black Peak scoria cone volcanoes (Nevada, U.S.A.)

Greg A. Valentine · Gordon N. Keating

Received: 11 October 2006 / Accepted: 29 January 2007 / Published online: 9 March 2007

Abstract We describe two small scoria cone volcanoes, Hidden Cone and Little Black Peak (ages between ~320–390 ka), in the Southwestern Nevada Volcanic Field and discuss their eruption mechanisms and inferences about their plumbing systems. Cone-forming pyroclastic deposits are consistent with eruptive styles ranging from Strombolian to violent Strombolian, and lavas emanated from near the bases of the cones. The volcanoes are monogenetic (rather than polycyclic, as allowed by previous geomorphic interpretations). Vents at each volcano appear to coincide with pre-existing normal faults, consistent with observations at older, deeply eroded volcanoes in the region. The existence of these two volcanoes on a topographically high area (particularly Hidden Cone) provides evidence for short feeder dike lengths (~500 m at the surface). We infer that this short length reflects the small length scale of the mantle source region that was tapped to feed each volcano.

Keywords Scoria cone · Dike · Southwest Nevada Volcanic Field

Introduction

Eruptive styles and the factors that control location of continental basaltic volcanoes and their vents are important from the perspective of predicting volcanic risk and for our overall understanding of basaltic magmatism and volcanic field evolution. Sporadic basaltic volcanism in the Southwestern Nevada Volcanic Field (SNVF; Fig. 1a) is of particular interest because of its potential impact on the proposed Yucca Mountain radioactive waste repository (excavated at depths of ~250–350 m below the surface) over the 10^4–10^6 year time scales for which repository performance must be estimated. Significant issues include eruptive styles, the length scale of shallow plumbing (dikes and conduits), and relationships of dikes and vents to pre-existing structures such as the normal faults that occur in Yucca Mountain (Crowe et al. 1983; Doubik and Hill 1999; Connor et al. 2000; Woods et al. 2002; Dartevelle and Valentine 2005; Gaffney and Damjanac 2006; Valentine and Krogh 2006; Valentine and Perry 2006).

The eight Quaternary scoria cone volcanoes in the SNVF (Fig. 1a) are important analogs for potential future volcanic activity that might intersect the repository; previous papers have described the physical volcanology of the five ~1 Ma volcanoes of Crater Flat (Valentine et al. 2006; note that SW and NE Little Cones, which are part of the Crater Flat group of Quaternary volcanoes, might have a somewhat younger age of ~780 ka, reflecting one $^{40}Ar/^{39}Ar$ age determination that has relatively small error) and of the ~80 ka Lathrop Wells volcano (Heizler et al. 1999; Valentine et al. 2005, 2007). Hidden Cone and Little Black Peak volcanoes (Figs. 1b and 2), the subject of this paper, have K–Ar and $^{40}Ar/^{39}Ar$ ages between ~320–390 ka (Fleck et al. 1996; Perry et al. 1998). Compositionally they straddle the basalt to trachybasaltic fields on an alkali-silica plot (Le Bas et al. 1986; Fleck et al. 1996) and are relatively phenocryst poor, with minor plagioclase and a few percent of olivine phenocrysts (mainly mm to sub-mm in size). We discuss inferred eruption and emplacement processes of the volcanic products, in comparison with

Editorial responsibility: J Stix

G. A. Valentine (✉) · G. N. Keating
Earth and Environmental Sciences Division,
Los Alamos National Laboratory,
Mail Stop D462,
Los Alamos, NM 87545, USA
e-mail: gav@lanl.gov

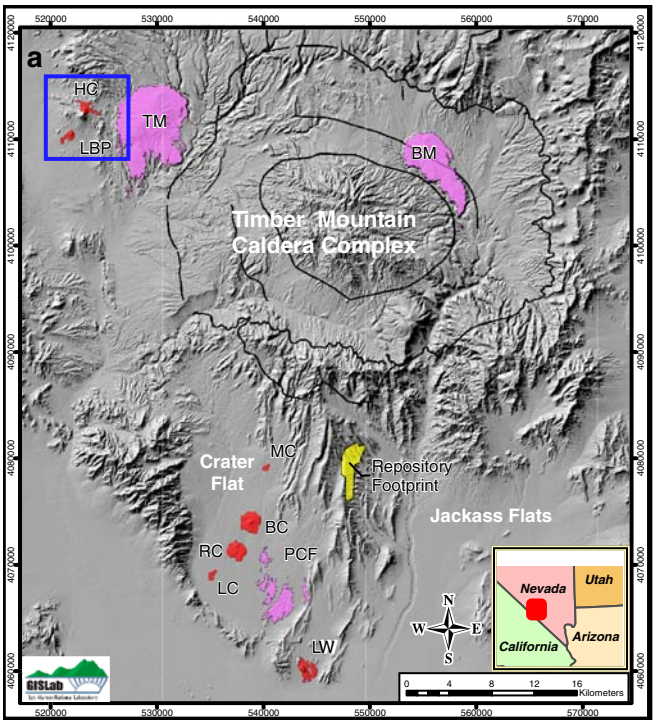

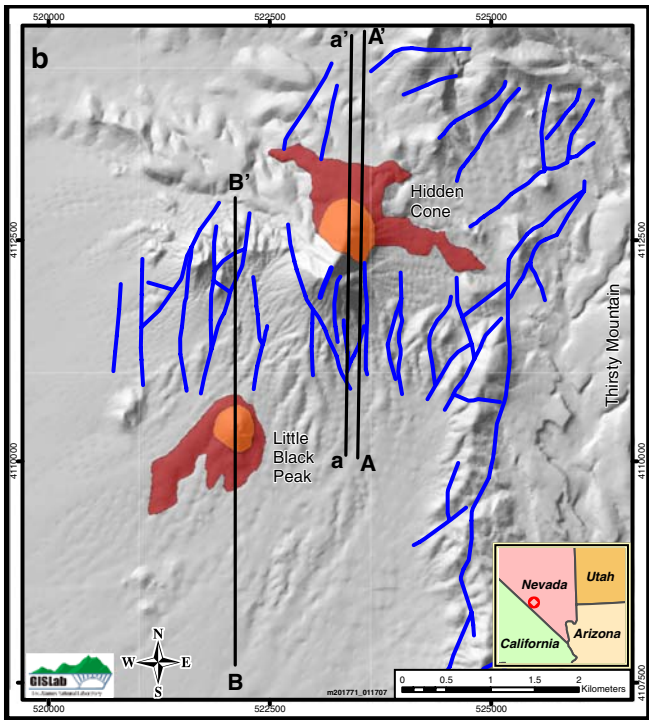

Fig. 1 **a** Pliocene (*magenta*) and Pleistocene (*red*) basaltic volcanoes in the Southwestern Nevada Volcanic Field (not including known or inferred buried volcanoes): Thirsty Mountain (*TM*), Pliocene Crater Flat (*PCF*), and Buckboard Mesa (*BM*), Makani (*MC*), Black Cone (*BC*), Red Cone (*RC*), SW and NE Little Cones (both labeled together as *LC*), Little Black Peak (*LBP*), Hidden Cone (*HC*), and Lathrop Wells (*LW*). Proposed high-level radioactive waste repository is indicated in *yellow*. *Solid black lines* represent margins of Miocene silicic calderas (Wahl et al. 1997). *Inset* shows location with respect to the southwestern United States. *Blue box* indicates location of Fig. 1b. **b** Detail of study area, showing scoria cones (*orange*) and lava fields (*red*). Major faults (*blue*) are modified from Slate et al. (1999). Lines a-a′, A-A′, and B-B′ are locations of topographic profiles shown in Fig. 4

other Quaternary volcanoes in the SNVF, and show that the locations of vents were controlled by pre-existing faults. Finally, we discuss implications of the relationships between volcano locations, faults, and topography with respect to the characteristic length scales of the deeper plumbing and magma source region.

Hidden Cone

Hidden Cone (Fig. 2a) is a scoria cone with two or three small lava fields, and an estimated total preserved volume of about 0.03 km^3. The scoria cone straddles the northeastern end of Sleeping Butte, a structural block of Miocene ignimbrite that rises ~230 m above the surroundings and has a summit ridge that is ~500 m long with a N-NE trend. Normal faults with oblique slip components extend across the east slopes of Sleeping Butte (Fig. 1b), displacing the ignimbrite successively downward to the east (Minor et al. 1998; Slate et al. 1999). The Hidden Cone deposits bury the northern extensions of the faults, and there is no visible displacement within those deposits, indicating that slip completely predates the volcano.

The cone has a small crater that is now breached on its east side by a gully that feeds a small outwash fan at the cone's base (Fig. 2a). The outer slopes of the cone are rilled, and a narrow zone of remobilized scoria and eolian material, typically deposited in small fans, circles the base of the cone to form a cone apron. Most of the cone slopes, including the inner crater slopes near the top of the butte, are composed of loose, vesicular scoria lapilli with blocky to fluidal and irregular (e.g., small ribbons) shapes, forming the upper cone facies. The lapilli most commonly have mm or smaller sized vesicles. These deposits are infiltrated with eolian sediment. The inner crater slopes have more abundant fluidal bombs typically 10–30 cm long, and scattered chunks of agglutinate that formed close to the vent and were later re-ejected. Some rounded bombs are coated with scoria lapilli that are imbedded on the bomb surfaces, suggesting that still-molten bombs that landed on the crater

Fig. 2 **a** Geologic map of Hidden Cone. Cone scoria and agglutinate ▶ units correspond to upper and lower cone facies, respectively, as discussed in the text. **b** Geologic map of Little Black Peak. Both maps use information from Crowe and Perry (1991), Fleck et al. (1996), Minor et al. (1998), and Slate et al. (1999), as well as our own observations

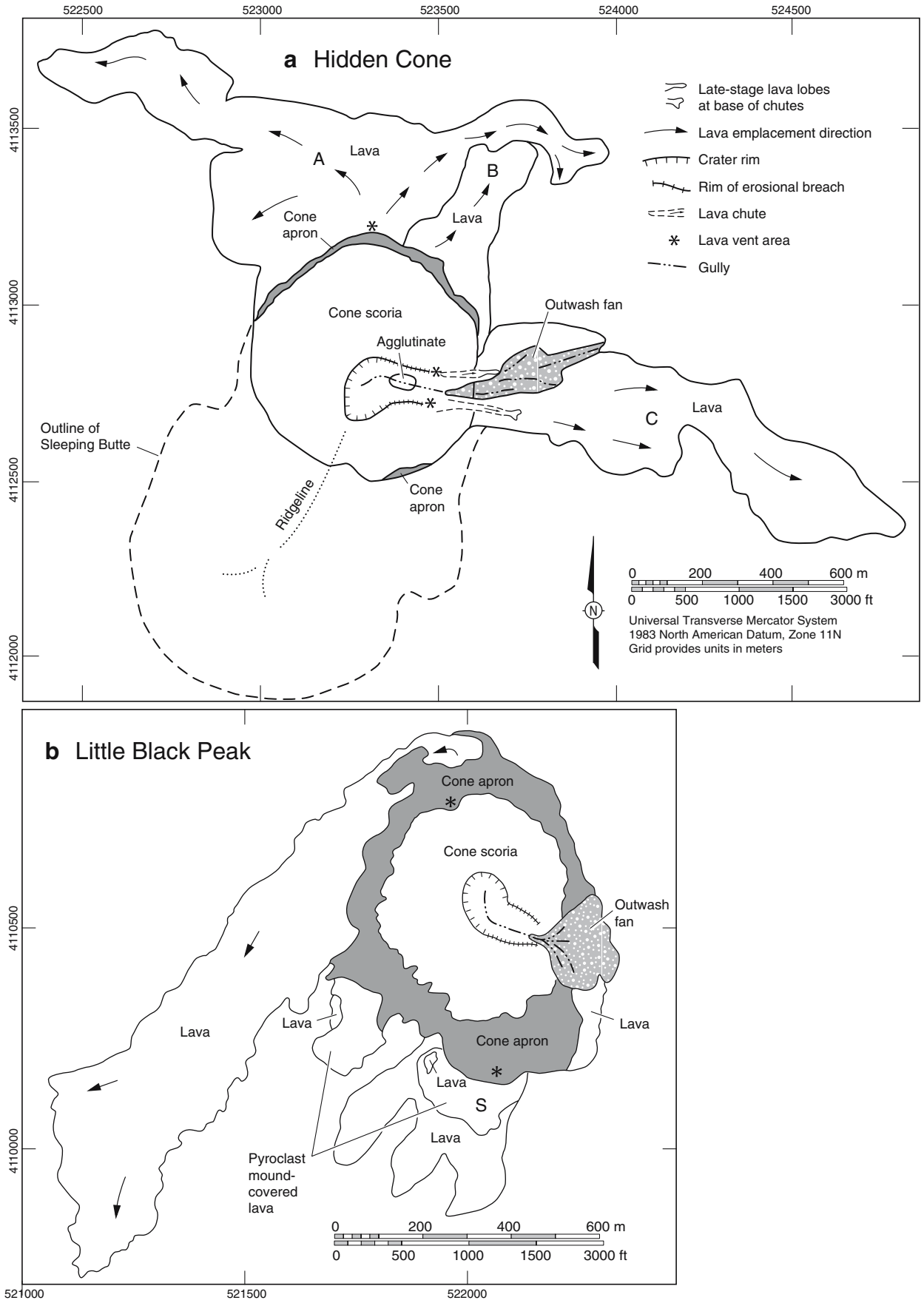
a Hidden Cone
Late-stage lava lobes at base of chutes
Lava emplacement direction
Crater rim
Rim of erosional breach
Lava chute
Lava vent area
Gully
A
Lava
B
Lava
Cone apron
Cone scoria
Outwash fan
Agglutinate
C
Lava
Outline of Sleeping Butte
Ridgeline
Cone apron
0 200 400 600 m
0 500 1000 1500 3000 ft
N
Universal Transverse Mercator System
1983 North American Datum, Zone 11N
Grid provides units in meters
522500
523000
523500
524000
524500
4113500
4113000
4112500
4112000
b Little Black Peak
Cone apron
Cone scoria
Outwash fan
Lava
Lava
Lava
Cone apron
Lava
S
Lava
Pyroclast mound-covered lava
0 200 400 600 m
0 500 1000 1500 3000 ft
4110500
4110000
521000
521500
522000

walls commonly rolled back toward the vent and accreted smaller clasts. The only in situ deposits in the cone are exposed in the gully between about 40–50 m below the cone summit. These deposits form crude beds of variably welded spatter and bombs that dip back into the butte (westward) at 10–20°. Most clasts in this lower cone facies are bomb-size with ropy to ragged surfaces, and spindle and ribbon shapes are abundant; many of these are ~1 m long. In contrast to the upper cone facies, the lower cone deposits have more abundant coarse vesicles 2 mm or greater in size.

Lavas that extend from the northern base of the cone flowed both westward and eastward. We have subdivided the northern lava field into two main units, A and B (Fig. 2a), following Minor et al. (1998). The northern flows probably vented from a bocca near the base of the cone that was subsequently covered by loose scoria of the upper cone facies. The surfaces of the A unit are subdued due to weathering and accumulation of eolian sediment, but still preserve some squeeze-ups and remnants of blocky texture. The lavas are composed of many stacked flow units, with upper (later) units commonly terminating inboard of the underlying unit, forming a surface that steps upward in a terrace-like manner toward the cone. Individual flow units range from about 2–4 m in thickness. The B unit is poorly exposed but is higher standing than most of the A unit and appears to be a highly brecciated lava with rafted cone material on its top. A limited exposure where unit B breccia appears to overlie unit A suggests that B was emplaced after A.

The eastern lava field (unit C on Fig. 2a) is similar to unit A and extends 1.3 km from the base of the cone. The field can be traced to two vent areas or boccas about 70 m up the cone flank, on either side of the gully that drains the crater. The northern bocca is preserved as a prow-shaped (pointing uphill) body of lava, up to 6 m wide and concentrically foliated, extending 10–15 m down slope. Vertical contacts with the surrounding scoria are parallel to concentric slabs (3–15 cm thick) within the lava, which are marked by shear zones containing shark's-tooth texture. Near the down slope end of the bocca, the vertical contacts relax to dip steeply (70°) inward, toward the axis. The transition from outward directed flow from the bocca to down slope flow is marked by the attitude of the basal contact of the lava, which becomes concordant with underlying scoria about 15 m down slope from the top of the bocca. Below this transition, the lateral margins of the lava are less constrained, and the flow widens and has increasingly jumbled jointing down slope. The southern bocca is not well preserved but its location is indicated by exposed outer margins of its channel that extend upslope into a subdued swale (~60 m wide) in the side of the cone. The channel is lined with alternating, dm-thick layers of lava and breccia that we infer record the passage of pulses of lava. Below the boccas, lavas flowed down channels or chutes to the base of the cone where they fed the eastern lava field. A small, late-stage lava lobe extends from the base of the southern channel, possibly representing rheomorphic remobilization of channel-lining material.

Little Black Peak

Little Black Peak (Fig. 2b), although at a lower altitude than Hidden Cone, is located on the front of the Tolicha Peak range block, emplaced on a veneer of alluvial fan deposits, between ridges of Miocene Tuff of Sleeping Butte and the Middle Rhyolite of Quartz Mountain (Slate et al. 1999; Minor et al. 1998). Numerous normal faults are mapped in the nearby ridges (Fig. 1b), but none is observed to cut Quaternary fan deposits near the base of volcano. The total volume of preserved eruptive material at Little Black Peak is 0.014 km^3.

The scoria cone forming Little Black Peak is about 400 m in diameter, slightly elongated north–south, and 70–100 m high. The cone is breached by an erosional gully to the east, forming a small outwash fan at the eastern base of the cone. Erosion of the cone surface has produced rills up to a meter deep and spaced ~10 m apart. The rills terminate downward in gullies between small, earlier-erosional-stage fans of the cone apron (intermediate stage of cone degradation illustrated in Valentine et al. 2006). The summit crater is an irregular bowl about 10 m deep with gently sloping sides covered by loose scoria lapilli, blocks, and bombs. The rim of the crater is a flat platform about 20 m wide; this might imply erosion of at least 5–6 m of the original height of the cone (assuming original 30° slopes), or it might reflect the original cone morphology. Bedded, partially welded scoria lapilli, blocks, and bombs are exposed in the walls of the breach about 6 m below the base of the crater. These beds dip ~30° NW, toward the crater. There is a marked difference in grain size of the loose pyroclasts between the south and north walls of the breach. On the south wall, red scoria lapilli blanket the walls of the gully, while on the north wall coarse lapilli to block- and bomb-size pyroclasts are dominant. The curving gully in the breach appears to follow this difference in grain size in the cone deposits.

Lavas erupted from the base of the cone in up to four locations; these lavas are similar to those at Hidden Cone. The western flow is the longest (1,500 m) and emanated from an inferred bocca in the northwest base of the cone (Fig. 2b; see also Crowe and Perry 1991). A slight depression in the cone slope and a concentration of m-size lava boulders with brecciated rinds marks the likely vent/bocca area. The flow thins away from this location to a 1–2-m high flow front at the northern extent. The west margin of this

flow is being eroded by an active wash, and several flow units produce a 10-m high stack. The surface topography is subdued, with dm-scale terraces topped with tight pavements and underlying eolian silt that forms a desert soil with a vesicular A horizon (McFadden et al. 1987, 1998; Valentine and Harrington 2006). A small lobe of lava on the east side of the cone forms a low (5–6 m) bench that is partially buried by the alluvial debris from the breach. This flow likely emanated from the eastern base of the cone. The south flank of the cone was the source of several other lava flows that formed three prominent benches at the cone base and thin tongues of lava on the desert floor, now partially covered by alluvium. These flows extend less than 400 m from the base of the cone. The lava and scoria platforms extend ~100 m from the base of the cone apron, with exposures of dense lava, lava breccia, and agglutinate around the margins (somewhat similar to lava unit B at Hidden Cone). A soil pit in the S platform (labeled S in Fig. 2b) exposes variably agglutinated scoria lapilli, blocks, and bombs to a depth of 1–2 m. The abundance of ropy and spindle bombs, along with the breccia and agglutinate exposures, indicates that the S platform, near the cone base, was a vent area for small lava flows. The coarse material might also be partly or wholly the result of rafting of cone material atop the lavas. The presence of the near-vent deposits on the S scoria platform in close proximity to the distinct package of fine-grained scoria lapilli on the upper southeast cone flank (exposed in the breach and contrasting with the coarser cone facies to the north) indicates that the southern sector of the cone may have been temporarily destroyed by rafting or vigorous lava effusion from the bocca related to S platform. Later stage, finer-grained eruptions from the main cone then healed the rafted sector and covered the lava vents with fallout deposits.

Interpretation and implications

The inferred eruptive styles of Hidden Cone and Little Black Peak volcanoes are consistent with the styles inferred for most of the Quaternary volcanoes in the Southwestern Nevada Volcanic Field. Although the pyroclastic facies in the interiors of the two cones are not as well exposed as the deeply incised Red Cone and Black Cone volcanoes (Valentine et al. 2006) or the actively quarried Lathrop Wells volcano (Valentine et al. 2005, 2007), the facies appear to be similar. In particular, Hidden Cone appears to have had a similar sequence of explosive styles as the Lathrop Wells volcano, namely an early phase of Strombolian activity (low, short-lived bursts of coarse ejecta caused by bursting of bubbles through the top of a slow-rising magma column), reflected in the lower cone facies, followed by a more energetic violent Strombolian phase that produced sustained eruption columns (hundreds of meters to ~10 km high) of well-fragmented, finely vesicular lapilli and ash as represented by the upper cone facies. Little Black Peak may have had a similar sequence of explosive styles, reflected in the contrasting deposit characteristics on either side of the erosional gully, although the relative timing of the styles is ambiguous. Unfortunately, the nature of any violent Strombolian tephra fallout deposits that might have extended beyond the immediate vicinities of the cones cannot be determined due to post-eruptive erosion. Lava-flow styles are also similar to those at other Quaternary volcanoes in the SNVF, with most effusion from breakouts or boccas low on the cone flanks (as opposed to the central crater of the scoria cones) and relatively low effusion rates (less than ~3 m^3/s using the relationship between flow length and effusion rate of Walker 1973). The lava fields at Hidden Cone and Little Black Peak are generally thinner than other Quaternary lava fields in SNVF (Valentine et al. 2006, 2007), but have similar flow morphologies (blocky surfaces, steep edges, squeeze-up structures, and stacked flow units). The relative thinness may simply be related to shorter effusion times, producing fewer stacked lava units and less inflation, for these smaller-volume volcanoes. The lava surfaces have evolved due to weathering, eolian sediment accumulation, and pedogenesis, to a stage (late Stage A of Wells et al. 1985) that is intermediate between those at Lathrop Wells and at Red and Black Cone volcanoes.

Crowe and Perry (1991) interpreted Hidden Cone to be polycyclic, with the latest eruption (corresponding to the upper cone facies) postdating the earlier (lower cone facies and lavas) eruptions by ~200–300 kyr (perhaps as young as Holocene). Later interpretations by Perry et al. (1998) allowed that Hidden Cone was equally likely to represent a monogenetic or a polycyclic volcano. Both Crowe and Perry (1991) and Perry et al. (1998) cited a lack of rilling on the cone slopes, in contrast with relatively advanced soil development on deposits around the base of the cone (cone apron deposits in Fig. 2a). They interpreted the main cone slopes to have been deposited by a relatively recent eruption compared to the deposits at the base of the cone, which were interpreted to be the apron of a much older cone that had not been completely buried by the more recent activity. Figure 3a demonstrates that the cone slopes are indeed rilled. Apron deposits at the base of the rilled slopes are composed of a remobilized mixture of scoria and of eolian sediment that is continuously accreting on the cone slopes as well as on the apron deposits themselves; this mixture, with its abundant fine sand and silt, results in more advanced soil development on the apron deposits compared to the cone slopes that are periodically eroded. In short, we did not observe any evidence that supports the possibility of Hidden Cone being polycyclic. The conclusion that the

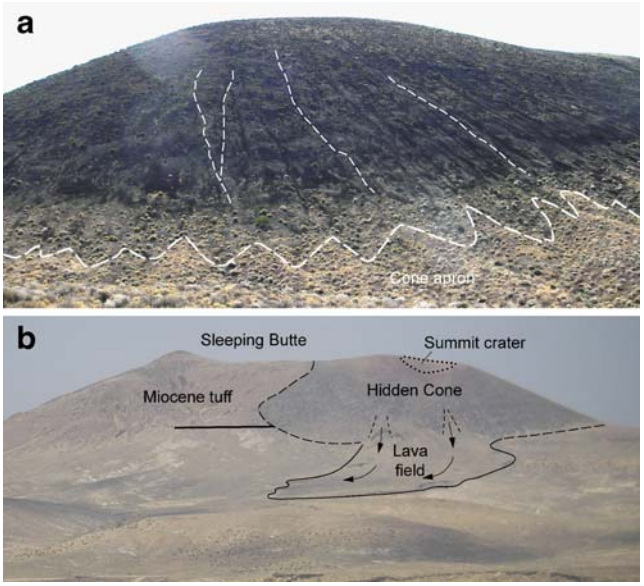

Fig. 3 **a** Photograph of the northwest side of Hidden Cone, showing rills (examples shown with *short-dash lines*) and cone apron deposits (*long-dash line*). **b** Photograph of east side of Sleeping Butte and Hidden Cone. Summit crater (*dotted line*), cone base (*long dash lines*), eastern lava flow field (*solid line*), and lava breakouts/chutes (*short dash lines*). *Arrows* indicate main lava flow directions. *Heavy solid line* shows approximate trace of a major normal fault in the lower part of the butte

volcanoes are monogenetic is consistent with results of K–Ar and paleomagnetic data reported by Fleck et al. (1996).

Field relationships suggest that vents at the two volcanoes coincide with pre-existing, approximately N–S trending, normal faults. The two boccas that fed the eastern lava field at Hidden Cone are roughly on trend with the projection of a north-striking fault; this fault is one of at least three oblique-slip faults along the east side of Sleeping Butte (Figs. 1b and 3b) that progressively drop the Miocene stratigraphic succession down to the east. The inferred bocca that fed the northern lava field at Hidden Cone is approximately due north of the summit crater; if the two are connected at depth by a dike, its orientation would parallel much of the structural grain of the area. Fleck et al. (1996) reached a similar conclusion regarding fault control for Hidden Cone. The main apparent vent areas at Little Black Peak (summit crater, northern lava bocca, and S platform) also approximately form a N–S trending alignment that could be related to pre-existing faults in underlying tuff bedrock, although the thin alluvial cover surrounding the cone precludes direct mapping of such faults into the cone. The N–S fault grain is inherited from an older stress field and is oblique to the modern (and presumed for the time the two volcanoes discussed here were emplaced) stress field that has a NW-directed least principal stress (σ_3), such that young dikes that are unaffected by pre-existing structures would have NE-trending strikes (Stock and Healy 1988). We have studied older (Miocene) basaltic volcanoes in the region that erupted through similar structural blocks, and where the shallow feeder systems (dikes and conduits) are exposed by erosion (Valentine and Krogh 2006; Keating et al. 2007); vents within each of these volcanoes ubiquitously coincide with pre-existing normal faults and, in some cases, were located on topographic highs. We suggest that Hidden Cone and Little Black Peak are younger examples of this phenomenon; however, it is not clear whether the eastern boccas at Hidden Cone represent discharge from a separate, fault-hosted (N–S trending) dike, or from radial dikes that propagated from the main conduit (beneath the pyroclastic vent) whose breakout location was influenced by the presence of a fault.

A line connecting Little Black Peak and Hidden Cone trends ~N30°E, perpendicular to the current orientation of σ_3 (Fleck et al. 1996). Previous authors (e.g., Perry et al. 1998; Connor et al. 2000) noted a similar pattern in the ~1 Ma volcanoes of Crater Flat, where individual volcanoes appear to have vented along ~N–S trending faults but at a larger scale the five volcanoes form a NE-trending alignment. One interpretation is that the Little Black Peak–Hidden Cone and the ~1 Ma Crater Flat alignments each were fed by one master dike with an orientation at depth that was perpendicular to σ_3, but that broke into segments that followed pre-existing faults at shallow depths. This interpretation would imply that the volcanoes along a given alignment erupted contemporaneously. Unfortunately, age dates do not have sufficient resolution to test this hypothesis and instead allow the possibility that volcanoes on a given alignment could have formed as separate monogenetic events over period of several 10s of kyr; the products of the volcanoes do not overlap each other, making it impossible to use stratigraphic relationships to test for relative timing. However, our studies at older, eroded basaltic volcanoes in the region suggest that vent alignments fed by a single master dike tend to have spacings between major vents on the order of 500–2000 m (commonly with overlapping eruptive products; Keating et al. 2007), while the alignments at Little Black Peak–Hidden Cone and in Crater Flat have vent spacings of ≥2.5 km (except for the ~400 m spacing between SW and NE Little Cones; Valentine et al. 2006). Thus we favor an interpretation wherein each volcano represents a temporally separate magmatic event within a longer pulse of activity.

There are three fundamental controls on the location of individual monogenetic basaltic volcanoes in continental settings: (1) Location and length scale of the mantle source region that is tapped to provide magma (magmatic footprint; Valentine and Perry 2006). (2) Topographic variations within the magmatic footprint, which can cause an ascending dike to break the surface at a low point where conduit flow is subsequently focused (Gaffney and Damjanac 2006). (3) Pre-existing structural weaknesses

such as faults or joints that reside within the projection of the magmatic footprint into the shallow crust (e.g., Valentine and Krogh 2006). Several studies indicate that dike propagation in continental basaltic fields is dominantly vertical, rather than dominantly horizontal as is often observed on the flanks of large shields or high-flux volcanic rift zones such as at Hawaii and Iceland (e.g., Delaney and Gartner 1997; Kuntz et al. 2002). Hidden Cone, and to a lesser degree Little Black Peak, support this conclusion, even though their feeder dikes are not exposed for direct observation. Both volcanoes erupted on topographically high areas. Hidden Cone, as mentioned above, has two potential vent alignments that are roughly parallel to faults in Sleeping Butte: one alignment is formed by the summit crater and the inferred bocca that fed the northern lava field, while the other alignment is formed by the two boccas that fed the eastern lava field. Vent locations compared to topography along transects that are coplanar with these two alignments (a-a′ and A-A′, respectively; Figs. 1b and 4a), as well as geologic mapping showing that no related dikes are present to the south or north of Hidden Cone, suggest that its feeder dike(s) must not have had a significant component of lateral propagation at shallow depths or else it would have vented in the immediately adjacent lower terrain. Similarly, the vertically ascending dike(s) must have been relatively short (~500–700 m) near the surface. A topographic profile (B-B′; Figs. 1b and 4b) through the inferred main vents at Little Black Peak (summit crater, northern lava bocca, and S platform) shows that this volcano is high relative to terrain to the south (and west, although not shown in Fig. 4b). The possibility that Little Black Peak's feeder dike propagated laterally toward the vent area from beneath the higher terrain to the north cannot be ruled out, although the dike (fissure) length that might be inferred from the vent locations is similar (~500 m) to that at Hidden Cone and suggests similar vertical emplacement of a short dike.

If an upward propagating dike has, to first order, a smooth, arcuate top, it is reasonable to infer that the dike length increases with depth compared the length where it intersects the Earth's surface. Although difficult to constrain, this length increase might be a factor of 2–3 based upon shapes of dikes in laboratory experiments (see, for example, Menand and Tait 2002. Note that vertical variations in host rock properties could complicate this simple assumption and it is also possible that the tip of a dike could propagate upward as irregular "fingers" rather than as a smoothly curving surface.). Assuming that the feeder dike(s) for Hidden Cone is on the order of ~1–2 km long at depth, we suggest that the inferred dike length is consistent with a characteristic length scale of the mantle source region that was tapped to feed the volcano. For example, this source length scale might have been ~0.7–1.8 km for a range of partial melting from 1–5% and allowing for a portion of non-erupted magma between 0–0.03 km^3 (The upper bound being equal to the erupted volume. Note, however, this bound is not directly quantifiable without knowledge of the feeder dike dimensions with depth, i.e., whether the dike is continuous all the way to the mantle source region or is pinched off, or whether it varies in length and width as it cuts through the full crustal

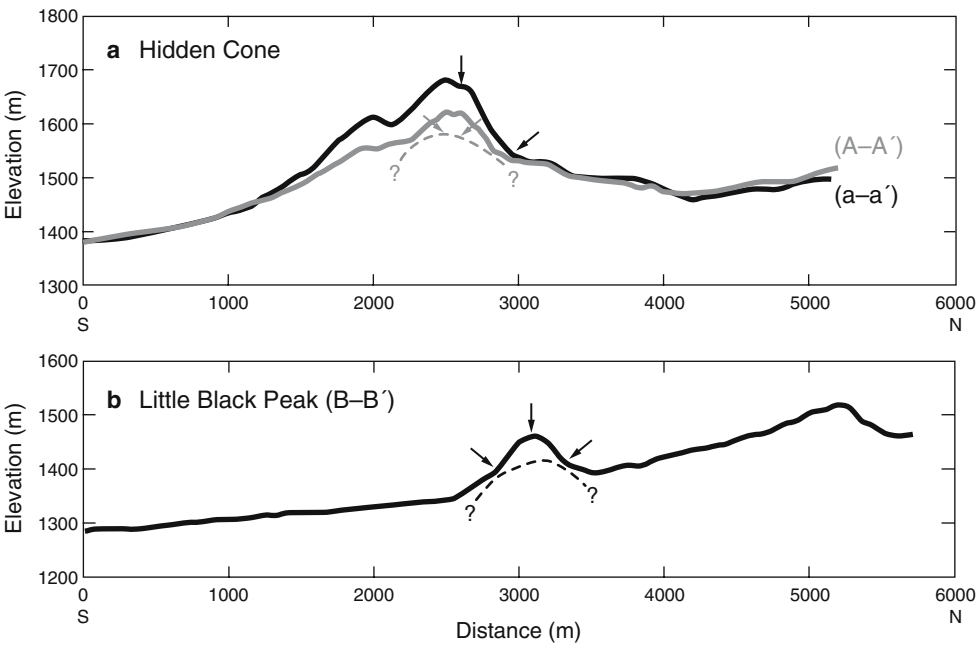

Fig. 4 Topographic profiles through **a** Hidden Cone (a-a′ and A-A′), and **b** Little Black Peak (B-B′). See Fig. 1b for locations of profiles. *Arrows* point to vents (either summit craters or lava boccas) intersected by each profile. *Dashed lines* represent inferred top edges of feeder dikes as constrained by vent locations and surrounding topography

section as mentioned above.). This length scale is estimated simply as the cube-root of the magma volume, correcting for percentage of melt or "porosity" in the source for each volcano, and thus assumes that the source that is tapped has a vertical thickness that is similar to its areal dimensions. This result is consistent with the notion proposed by Valentine and Perry (2006) that length scales of surface eruptive features are directly related to the length scales (magmatic footprints) of the magma source for each volcano in a basaltic field.

The proximity (~4 km) of Little Black Peak and Hidden Cone to the 4.6 Ma Thirsty Mountain shield volcano (Fleck et al. 1996) suggests the possibility that the underlying lithospheric mantle source in this area has a slightly different composition that makes it more prone to partial melting than surrounding rocks, and therefore a site to which volcanism may return over long periods of time. Given the different length scales and degrees of partial melting that produced the three volcanoes, it might be possible to constrain mantle compositional variations on the scale of the entire cluster (Thirsty Mountain, Hidden Cone, and Little Black Peak) as well as within the cluster, following the suggestion of Valentine and Perry (2006).

Acknowledgements This work was supported as part of the volcanic risk studies for the U.S. Department of Energy's Yucca Mountain Project. We thank Frank Perry for his insights and discussion and for reviewing the manuscript, Don Krier for reviewing the manuscript, and Mike Cline for his management support of the work. Rick Kelley performed GIS volume calculations for Hidden Cone and Little Black Peak and developed Fig. 1, and Andrea Kron did the artwork for Figs. 2, 3 and 4. Comments and suggestions by C. Connor and an anonymous reviewer greatly helped to improve the paper.

References

Connor CB, Stamatakos JA, Ferrill DA, Hill BE, Ofoegbu GI, Conway FM, Sagar B, Trapp J (2000) Geologic factors controlling patters of small-volume basaltic volcanism: Application to a volcanic hazards assessment at Yucca Mountain, Nevada. J Geophys Res 105:417–432

Crowe BM, Perry FV (1991) Preliminary geologic map of the Sleeping Butte volcanic centers. Los Alamos Nat Lab Rep LA-12101-MS

Crowe BM, Self S, Vaniman D, Amos R, Perry F (1983) Aspects of potential magmatic disruption of a high-level radioactive waste repository in southern Nevada. J Geol 91:259–276

Dartevelle S, Valentine GA (2005) Early-time multiphase interactions between basaltic magma and underground openings at the proposed Yucca Mountain radioactive waste repository. Geophys Res Lett 32:L22311. DOI 10.1029/2005GL024172

Delaney PT, Gartner AE (1997) Physical processes of shallow mafic dike emplacement near the San Rafael Swell, Utah. Geol Soc Am Bull 109:1177–1192

Doubik P, Hill BE (1999) Magmatic and hydromagmatic conduit development during the 1975 Tolbachik eruption, Kamchatka, with implications for hazards assessment at Yucca Mountain, NV. J Volcanol Geotherm Res 91:43–64

Fleck RJ, Turrin BD, Sawyer DA, Warren RG, Champion DE, Hudson MR, Minor SA (1996) Age and character of basaltic rocks of the Yucca Mountain region, southern Nevada. J Geophys Res 101:8205–8227

Gaffney ES, Damjanac B (2006) Localization of volcanic activity: topographic effects on dike propagation, eruption and conduit formation. Geophys Res Lett 33:L14313. DOI 10.1029/2006GL026852

Heizler MT, Perry FV, Crowe BM, Peters L, Appelt R (1999) The age of the Lathrop Wells volcanic center: an $^{40}Ar/^{39}Ar$ dating investigation. J Geophys Res 104:767–804

Keating GN, Valentine GA, Krier DJ, Perry FV (2007) Shallow plumbing systems for small-volume basaltic volcanoes. Bull Volcanol

Kuntz MA, Anderson SR, Champion DE, Lanphere MA, Grunwald DJ (2002) Tension cracks, eruptive fissures, dikes, and faults related to late Pleistocene-Holocene basaltic volcanism and implications for the distribution of hydraulic conductivity in the eastern Snake River Plain, Idaho. Geol Soc Am Spec Pap 353:111–133

Le Bas MJ, Le Maitre RW, Streckeisen A, Zanettin BA (1986) Chemical classification of volcanic rocks based on the total alkali-silica diagram. J Petrol 27:745–750

McFadden LD, Wells SG, Jercinovich MJ (1987) Influences of eolian and pedogenic processes on the origin and evolution of desert pavements. Geology 15:504–508

McFadden LD, McDonald EV, Wells SG, Anderson K, Quade J, Forman SL (1998) The vesicular layer and carbonate collars of desert soils and pavements: formation, age, and relation to climate change. Geomorphology 24:101–145

Menand T, Tait SR (2002) The propagation of a buoyant liquid-filled fissure from a source under constant pressure: An experimental approach. J Geophys Res 107:2306. DOI 10.1029/2001JB000589

Minor SA, Orkild PP, Sargent KA, Warren RG, Sawyer DA, Workman JB (1998) Digital geologic map of the Thirsty Canyon NW Quadrangle, Nye CO., Nevada. US Geol Surv Open File Rep 98–623

Perry FV, Crowe BM, Valentine GA, Bowker LM, eds. (1998) Volcanism studies: final report for the Yucca Mountain Project. Los Alamos Natl Lab Rep LA-13478-MS

Slate JL, Berry ME, Rowley PD, Fridrich CJ, Morgon KS, Workman JB, Young OD, Dixon GL, Williams VS, McKee EH, Ponce DA, Hildebrand TG, Swadley WC, Lundstrom SC, Ekren EB, Warren RG, Cole JC, Fleck RJ, Lanphere MA, Sawyer DA, Minor SA, Grunwald DJ, Laczniak RJ, Menges CM, Yount JC, Jayko AS (1999) Digital geologic map of the Nevada Test Site and vicinity, Nye, Lincoln, and Clark Counties, Nevada, and Inyo County, California. US Geol Surv Open-File Rep 99-554-A

Stock JM, Healy JH (1988) Stress field at Yucca Mountain, Nevada. US Geol Surv Bull 1790:87–93

Valentine GA, Harrington CD (2006) Clast size controls and longevity of Pleistocene desert pavements at Lathrop Wells and Red Cone volcanoes, southern Nevada. Geology 34:533–536, DOI 10.1130/G22481.1

Valentine GA, Krogh KEC (2006) Emplacement of shallow dikes and sills beneath a small basaltic volcanic center—the role of pre-existing structure (Paiute Ridge, southern Nevada, USA). Earth Planet Sci Lett 246:217–230

Valentine GA, Perry FV (2006) Decreasing magmatic footprints of individual volcanoes in a waning basaltic field. Geophys Res Lett 33:L14305. DOI 10.1029/2006GL026743

Valentine GA, Krier D, Perry FV, Heiken G (2005) Scoria cone construction mechanisms, Lathrop Wells volcano, southern Nevada. Geology 33:629–632

Valentine GA, Perry FV, Krier D, Keating GN, Kelley RE, Cogbill AH (2006) Small-volume basaltic volcanoes: eruptive products and processes, and post-eruptive geomorphic evolution in Crater

Flat (Pleistocene), southern Nevada. Geol Soc Am Bull 118:1313–1330. DOI 10.1130/B25956.1

Valentine GA, Krier DJ, Perry FV, Heiken G (2007) Eruptive and geomorphic processes at the Lathrop Wells scoria cone volcano. J Volcanol Geotherm Res 161:57–80. DOI 10.1016/j.jvolgeores. 2006.11.003

Wahl RR, Sawyer DA, Minor SA, Carr MD, Cole JC, Swadley WC, Laczniak RJ, Warren RG, Green KS, Engle CM (1997) Digital geologic map database of the Nevada Test Site area, Nevada. U S Geol Surv Open File Rep 97–140

Walker GPL (1973) Lengths of lava flows. Phil Trans R Soc Lond Ser A 274:107–118

Wells SG, Dohrenwend JC, McFadden LD, Turin BD, Mahrer KD (1985) Late Cenozoic landscape evolution on lava flow surfaces of the Cima volcanic field, Mojave Desert, California. Geol Soc Am Bull 96:1518–1529

Woods AW, Sparks S, Bokhove O, LeJune A-M, Connor CB, Hill BE (2002) Modeling magma-drift interaction at the proposed high-level radioactive waste repository at Yucca Mountain, Nevada, USA. Geophys Res Lett 29:1641. DOI 10.1029/2002GL014665